



Limiting High Frequency Longitudinal Impedance of an Inductive Pick-Up by a Thin Metallic Layer

Marek GASIOR, CERN



Abstract. An Inductive Pick-Up (IPU) was developed to measure the position and current of an electron beam of the Third CLIC Test Facility (CTF3) Drive Beam Linac. The pick-up construction is similar to a wall current monitor, but the pick-up inner wall is divided into 8 electrodes, each of which forms the primary winding of a toroidal transformer. The beam image current component flowing along each electrode is transformed to a secondary winding, connected to an output. The continuity of the vacuum chamber is taken care of by a ceramic insertion surrounded by the electrodes. The insertion is titanium coated on the inside and the end-to-end resistance of the layer is chosen in such a way that within the IPU bandwidth the image current flows over the electrodes. For higher frequencies the current is conducted by the coating to limit the longitudinal impedance of the device in the GHz range. This paper describes a simple electric network model, which was used to simulate the influence of the coating and to optimize its resistance. The model is built from sections of ideal transmission lines and resistors and is suitable for SPICE simulations. Results of measurements and simulations are compared.

Inductive Pick-Up of CTF3

The IPU front view longitudinal cross-section is shown in **Fig. 2** with focus on the elements important for the flow of the beam image current. The current enters the structure from the left by the rotatable flange and it continues through the bellows and the section of a stainless steel pipe. Then start two competing current paths: one by the screws and electrodes and the second through the ceramics collars and the titanium coating. The electrode path is of low resistance but significant inductance corresponding to the electrode internal diameter step while the path over the coating has much higher resistance and a small inductance. The image current passes over the path of smaller impedance for a given frequency. Thus, for low frequencies, the whole current passes along the electrodes, and for very high frequencies – over the coating. The threshold frequency is determined by impedances of the two paths and their frequency dependence.

The device senses only the beam image current passing through the transformers, so the alternative path of the coating introduces a high frequency limit for the current seen by the IPU. The frequency for which the electrode current drops by 3 dB is referred to as the electrode current cut-off f_{CE} .

The goal was to choose the coating resistance to the lowest possible value, but without significant deterioration of the device bandwidth. For this, a model was created allowing evaluation of f_{CE} , whose value should lie already beyond the IPU bandwidth and cannot be measured directly.

Longitudinal impedance Z_{\parallel}

When the image current has to pass over a diameter larger than that of the beam pipe, this perturbation inserts an inductive component into the longitudinal impedance Z_{\parallel} . The component increases linearly with frequency, also beyond the high cut-off frequency of the device. Taking the IPU of CTF3 as an example, the pick-up gives useful signals up to some 250 MHz but, since the CTF3 beam consist of electron bunches only 5 ps long (paced at a 1.5 GHz rate), the beam energy bandwidth extends beyond 100 GHz. With the geometry shown in **Fig. 1** and without the coating, $|Z_{\parallel}|$ from the electrode diameter step only would have been about 30 Ω at 1.5 GHz, 60 Ω at 3 GHz and 600 Ω at 30 GHz. The coating of end-to-end resistance of about 10 Ω puts a limit for Z_{\parallel} in the GHz range.

The coating limits the high frequency Z_{\parallel} , but, as stated before, also restricts the IPU bandwidth. The model presented in the paper was used to predict the optimal layer resistance.

Usually Z_{\parallel} of a device is estimated with so called wire method, where the device under test (DUT) constitutes a part of a measurement coaxial line. A signal is applied to the line and its drop along the structure is measured.

The Z_{\parallel} value is evaluated from the drop, which in the frequency domain can be derived from the device scattering matrix transmission coefficient S_{21} , measured with a network analyzer. To remove the setup dependency, a similar measurement is done, where the DUT is replaced by an equivalent length of the setup pipe.

In this paper Z_{\parallel} is calculated as

$$Z_{\parallel} = -2Z_L \ln \left(\frac{S_{21}}{S_{21R}} \right) \quad (1)$$

where Z_L is the impedance of the setup coaxial line, S_{21} is the S-matrix transmission coefficient of the setup with DUT, and S_{21R} is the corresponding result of the reference measurement.

An IPU Z_{\parallel} model

A simplification of the IPU cross-section of **Fig. 2** is shown in **Fig. 3** together with the wire method coaxial line. The structure is assumed to be axially symmetrical and only elements carrying the image current are taken into account. The following simplifications were done:

- The gaps between electrodes are neglected and all electrodes are considered as one cylinder (the electrodes cover 74 % of the circumference).

- The transformers and their screws are not taken into account as parts of the electrode current path, which is important only for frequencies below f_{CE} , i.e. some 300 MHz.

- The collars of the ceramic insertion are considered as short with respect to the ceramics length and their length is absorbed into that of the ceramics.

One can recognize three coaxial structures, each corresponding to one propagation mode in the IPU wire method measurement setup. An electrical model of the structure of **Fig. 3** is shown in **Fig. 4**, with one transmission line corresponding to each propagation mode. The lines are divided into short sections to model coupling between them and the coating resistance.

The line impedances are calculated as

$$Z_{COAX} = \frac{Z_0}{2\pi\sqrt{\epsilon_r}} \ln \left(\frac{d_2}{d_1} \right) \quad (2)$$

where d_2 and d_1 are the external and internal diameters of the corresponding structure, ϵ_r is the relative permittivity of the insulator and Z_0 is the characteristic impedance of vacuum. The coaxial structures are the following:

- The beam pipe line of impedance Z_L is defined by the diameter d_A of the inner conductor and d_B of the beam pipe.
- Impedance Z_I corresponds to the coaxial line formed by the titanium coating shell of diameter d_B and the outer surface diameter d_C of the alumina ceramics.
- Impedance Z_T corresponds to the air gap between the ceramics outer surface of diameter d_C and the electrodes of internal diameter d_D .

Dimensions of the mechanical model of **Fig. 3** are listed in **Tab. 1** and **Tab. 2** includes parameters of the electrical model of **Fig. 4**.

The line electrical lengths are calculated as the signal time of flight through the corresponding medium.

Tab. 1. Parameters of the mechanical model of Fig. 3.

Name	Value	Comments
l	95 mm	structure length
d_A/d_B	17.4 / 40 mm	central conductor / beam pipe diameter
d_C/d_D	48 / 49 mm	ceramics outer / electrode inner diameter

Tab. 2. Parameters of the electrical model of Fig. 4.

Name	Value	Comments
Z_L/t_L	50 Ω / 320 ps	main line impedance / length
Z_I/t_I	3.6 Ω / 880 ps	ceramics line impedance / length
Z_T/t_T	1.2 Ω / t_T	air line impedance / length
R_{SM}	11.2 Ω	Ti layer end-to-end resistance (measured)
N	512	cell number
R_{SM}	10 k Ω	formal requirements of the simulator

Simulations and measurements

The IPU model of **Fig. 4** with parameters as in **Tab. 2** was simulated with a SPICE simulator. The results are compared to corresponding measurements in the following figures.

As plotted in **Fig. 5**, the wire method simulation results fit well to the measurements, except for an important discrepancy of the imaginary parts for frequencies beyond 1 GHz and some undulations of the curves. The undulations are likely to be caused by small IPU details, which were not simulated at all and/or setup imperfections.

The imaginary part difference can be explained by a finite mechanical precision of the setup. Beyond 1 GHz the Z_{\parallel} imaginary part was small and, due to that, sensitive to all phase shifts between the reference and IPU measurements. The discrepancy can be removed by supposing 1 ps of an additional delay (i.e. 0.3 mm of a mechanical offset) between the reference and IPU measurements.

The measurements were done up to 3 GHz, beyond which waveguide modes in the setup render results meaningless. The simulations could be done up to 30 GHz, a frequency at which the length of the model cell was still negligible.

In **Fig. 6** there are shown time domain reflectometry (TDR) measurements of the wire method setup. The reflection corresponding to the IPU (or its reference replacement) starts from 0 ns. The IPU reflection has a “rise time” and a “fall time” due to the fact that the high frequency components of the image current flow over the coating and do not see the impedance step corresponding to the electrode diameter change.

The simulation results fit well to the measurements, except for some irregularities on the measurement curves. The following imperfections can be recognized:

- The bump before 0 ns, seen on both the IPU and reference measurements, corresponds to the bellows.
- The periodic ripples correspond to diameter changes of about 0.3 mm (calculated using (2) and measured with a slide caliper) of the setup central conductor (machining imperfections).
- The fastest undulations of the smallest amplitude and of frequency of a dozen of GHz, are believed to result from waveguide modes in the setup.

For direct observation of the coating influence on the electrode current beyond the IPU high cut-off frequency, the IPU was converted into a wall current monitor (WCM). The transformer and screw of each electrode were replaced by a “sandwich” of 30 SMD 51 Ω resistors (size 1206) soldered vertically next to each other. Each electrode was connected to the resistors by 10 small RF contacts. Electrodes were combined in pairs and the common signal connected to an output. The measured WCM normalized output voltage is plotted in **Fig. 7**, together with the corresponding simulated voltage and the electrode current I_E . The WCM was simulated by a circuit as in **Fig. 4**, with the electrode current probing network consisting of a resistance of 0.21 Ω (240 51 Ω resistors in parallel) in series with a parasitic inductance of 35 pH.

From the electrode current curve, f_{CE} can be estimated to be 320 MHz. Measured and simulated WCM output voltages have 3 dB cut-offs slightly higher, due to the inductive part of the probing network.

Conclusions

A simple model was built to predict the influence of a thin metallic layer on the longitudinal impedance of an inductive pick-up. The model consists of ideal delay lines and resistances and was simulated using a SPICE simulator. As was verified with measurements in the frequency and time domains, the optimal resistance of the coating and its behavior were successfully anticipated.

The effect of limiting the IPU output signal bandwidth by the metallic layer is not related to the skin effect. The IPU titanium layer of end-to-end resistance of about 10 Ω and resistivity of 54 $\mu\Omega\cdot\text{cm}$ has a theoretical thickness of some 40 nm, which corresponds to the skin depth in titanium at frequencies in the terahertz range.

The coating can be considered as a small impedance bypass for the higher impedance image current path over the IPU electrodes. This bypass limits the pick-up longitudinal impedance in the GHz range and introduces a high cut off frequency for the device output signals.

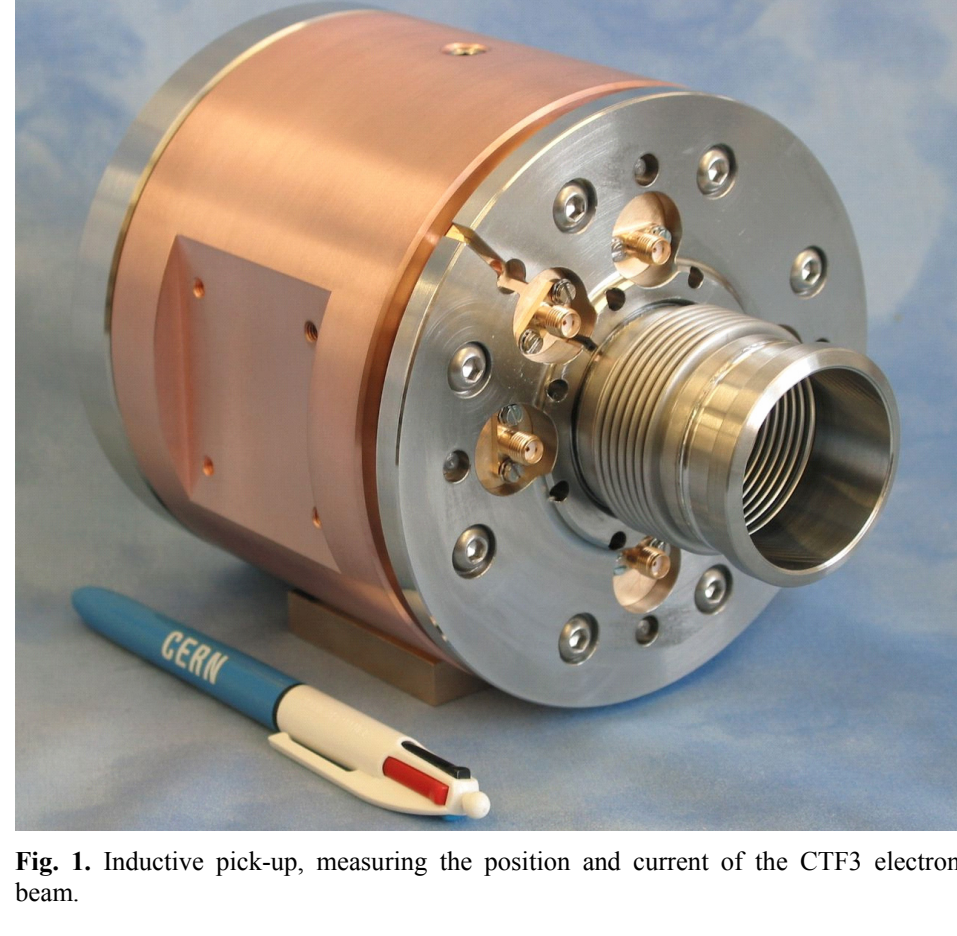


Fig. 1. Inductive pick-up, measuring the position and current of the CTF3 electron beam.

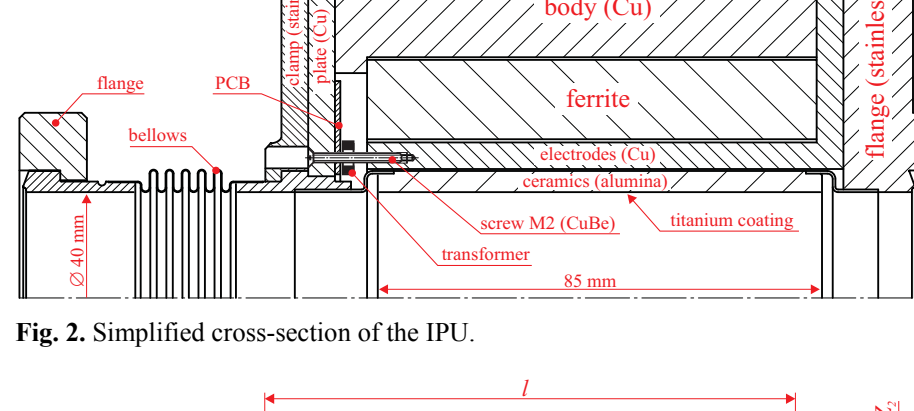


Fig. 2. Simplified cross-section of the IPU.

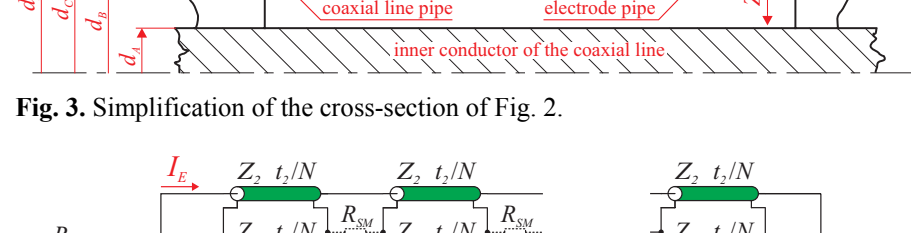


Fig. 3. Simplification of the cross-section of Fig. 2.

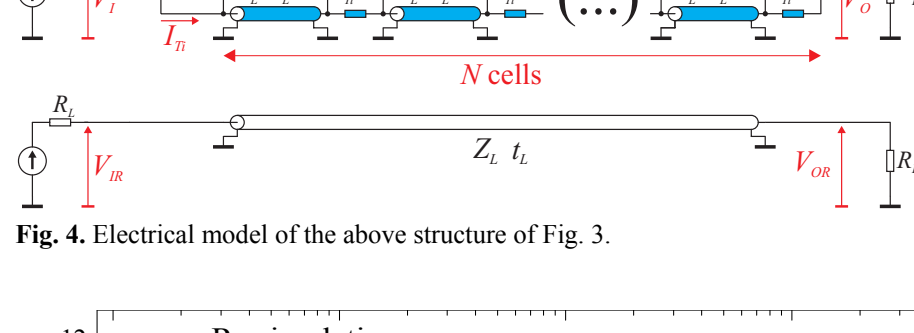


Fig. 4. Electrical model of the above structure of Fig. 3.

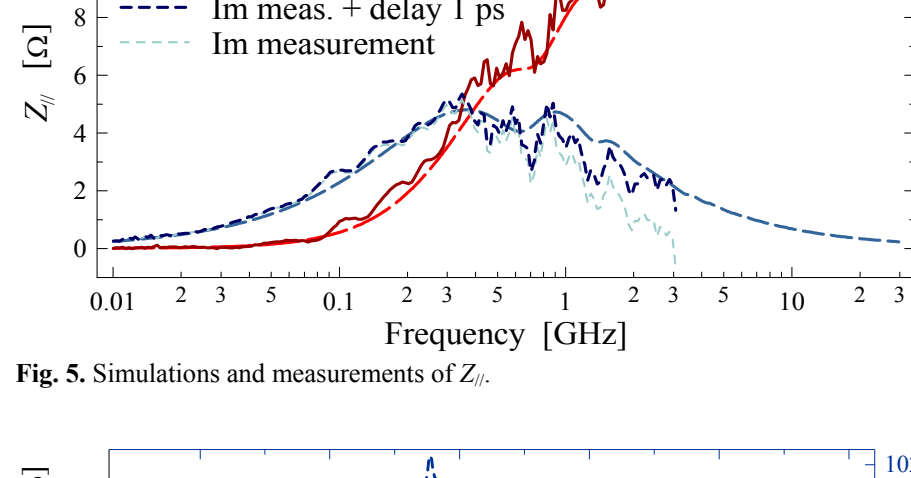


Fig. 5. Simulations and measurements of Z_{\parallel} .

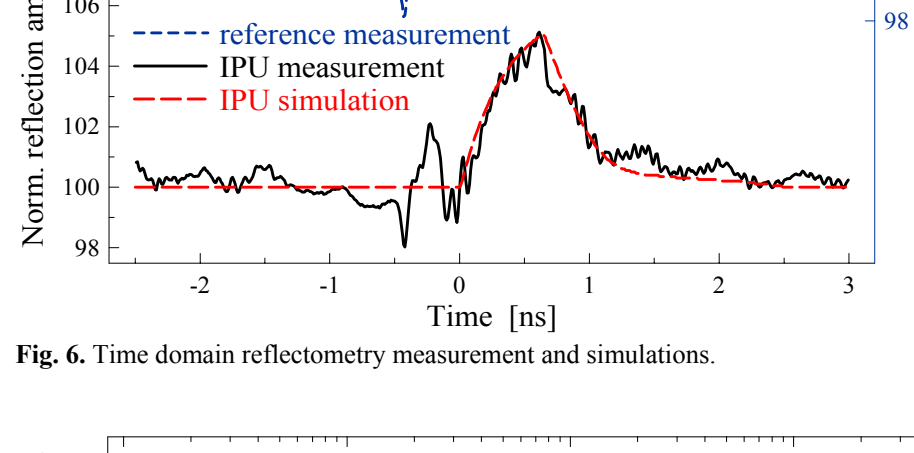


Fig. 6. Time domain reflectometry measurement and simulations.

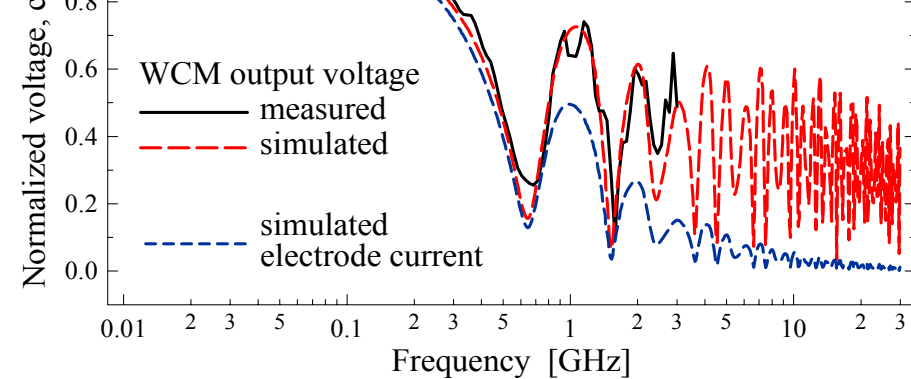


Fig. 7. Simulations and measurements of the IPU converted to a wall current monitor.